P H Y S I C A L   R E V I E W   L E T T E R S

☞

Observation of Slip Flow in Thermophoresis

Franz M. Weinert and Dieter Braun[*]

*Systems Biophysics, Ludwig Maximilians Universität München,
Amalienstrasse 54, 80799 München, Germany*

Two differing theories aim to describe fluidic thermophoresis, the movement of particles along a temperature gradient. While thermodynamic approaches rely on local equilibrium, hydrodynamic descriptions assume a quasi-slip-flow boundary condition at the particle's surface. Evidence for slip flow is presented for the case of thermal gradients exceeding $(aS_T)^{-1}$ with particle radius a and Soret coefficient S_T. Thermophoretic slip flow at spheres near a surface attracts or repels tracer particles perpendicular to the thermal gradient. Moreover, particles mutually attract and form colloidal crystals. Fluid dynamic slip explains the latter quantitatively.

Thermophoresis in water moves particles and molecules along a temperature gradient [1–3]. Typically, the particle velocity v is assumed to be a linear function of the temperature gradient ∇T: $v = -D_T \nabla T$, with the thermophoretic mobility $D_T = S_T D$, where the Soret coefficient is S_T and the diffusion coefficient is D. Several competing models have been proposed to describe the microscopic cause [4–17]. Recent experiments aim to distinguish between the models [18–21].

For small temperature gradients, the thermophoretic movement of polystyrene beads and DNA has been predicted quantitatively in the limit of a thin Debye layer, which is given by $a > 3\lambda$, where a is the hydrodynamic radius and λ is the Debye shielding length [8,10]. It was argued that the movement is the result of local equilibration driven by the thermal fluctuations of the particles [4–10]. However, such a local equilibrium model is expected to break down for thermal gradients exceeding the following condition [7–9]:

$$\nabla T > D/aD_T. \quad (1)$$

At larger thermal gradients, Marangoni-like quasislip on the particle surface is likely to dominate [11–17]. However, this regime is experimentally difficult to access. We devised two experimental strategies. In both cases, a cooling solid wall created a strong thermal gradient in the adjacent water film perpendicular to the surface. We probed the slip flow near the beads with smaller tracer particles, and we investigated how the hydrodynamic interaction between equal-sized particles leads to mutual attraction parallel to the surface.

In both cases, we found particle movement parallel to the wall although an insufficiently strong thermal gradient exists along this direction to cause the observed behavior. These findings cannot be explained with a local equilibrium approach, as the energy gradient parallel to the solid support is not sufficient to create the particle movement. However, the hydrodynamic interaction of the thermophoretic slip flow, which is deflected by the solid support, is

responsible for the observed particle movement, as shown below.

At a gradient smaller than the criterion from Eq. (1), particle fluctuations dominate, and no attraction or tracer movement parallel to the wall is found. This does not contradict an explanation based on thermophoresis with local equilibrium [7,8,10]. Our finding of fluid flow at strong thermal gradients points towards an interesting transition in thermophoresis near the thermal gradient given by Eq. (1).

Materials and methods.—Water was homogeneously heated in a thin chamber (10–25 μm) by an infrared laser scanning microscope (1455 nm, 300 mW; for details, see [22]). The laser was uniformly scanned across a rectangular area using a moderately focused beam (diameter 80 μm). The horizontal chamber temperature was imaged with a fluorescent dye [8,9] and checked for homogeneity. The vertical thermal gradient is derived from thermal conductivities of the chamber materials: insulating plastic on top ($\lambda = 0.16$ W/mK) and cooling sapphire at the bottom ($\lambda = 34$ W/mK). Typically, thermal gradients in the range of 0.2–0.7 K/μm are generated at the sapphire surface, and the fluid temperature is increased by less than 5 K. To confirm that optical trapping effects were absent, we used heavy water which is 100-fold less absorbing than water. In this system, the thermal gradients are equally reduced. All observed effects were reversible; after switching off the heating, the particles diffused freely again.

Tracer particle attraction and repulsion (Fig. 1).—We used small tracer particles (0.5 μm diameter, F-8888, Molecular Probes) to probe the possible fluid flow in the vicinity of larger particles (10 μm diameter). The latter were made from either polystyrene (F13838, Molecular Probes) or silica (PSI-10.0, Kisker) which show a positive and negative Soret coefficient under these conditions, respectively. The tracer particles ($S_T = 8.9$ K^{-1}) are also subjected to downward thermophoresis in a thermal gradient of $\nabla T = 0.24$ K/μm in a 25 μm thick chamber filled with saline-sodium citrate buffer (15 mM NaCl and
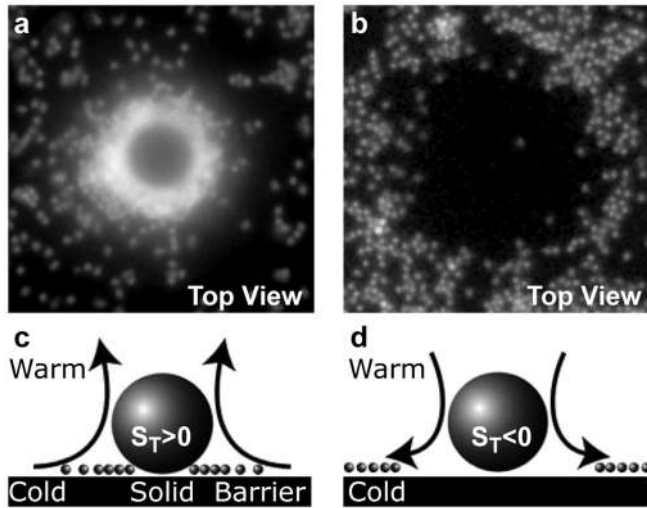
FIG. 1.   The slip flow induced by a temperature gradient across
particles with a diameter of 10 μm attracts or repels tracer
particles of diameter 0.5 μm. The direction of the flow depends
on the sign of the Soret coefficient of the large particle. (a) Poly-
styrene beads with $S_T > 0$ attract the tracer particles. (b) Silica
spheres with $S_T < 0$ repel them. (c),(d) Schematic side view of
the flow induced accumulation (depletion) of the tracer particles.

1.5 mM sodium citrate at pH 7.8) (Fig. 1). Tracer particles
accumulated near a 10 μm polystyrene particle, where an
upward directed slip flow was expected. The tracer parti-
cles were depleted from the area around the 10 μm silica
particles, which had a negative Soret coefficient, thus
indicating a downward slip flow [Figs. 1(c) and 1(d)].

Crystallization (Fig. 2).—In the above experiment, the
10 μm particles sedimented due to their weight. Smaller
particles with a positive Soret coefficient can be moved to
the cold surface by the thermal gradient. As a result of their
surface-generated slip flows, the particles subsequently
attract one another [Fig. 2(a)]. To probe this, we imaged
1 μm diameter polystyrene particles, which normally ex-
perience repulsive interactions with each other (10 pM,
F-8823, Molecular Probes) in 100 μM tris(hydroxy-
methyl)aminomethane hydrochloride buffer (pH 7.8) in-
side a 10 μm thin plastic-sapphire chamber. Without
thermal gradients, the particles diffused freely with a sedi-
mentation length of $L = kT/F_{pot} = 15$ μm, where F_{pot} is
the gravitational force [Fig. 2(c), inset]. After switching on
a thermal gradient of 0.65 K/μm [Fig. 2(b)], the thermo-
phoretic drift decreased the sedimentation length to below
$L = 1/(S_T \nabla T) = 100$ nm. As the particles reached the
surface, they were attracted to one another within inter-
particle distances of several micrometers and formed two-
dimensional crystals [Fig. 2(c)].

To exclude influences of optical effects induced by the
laser, we externally applied the temperature gradient by
cooling the outer top of an all-glass chamber to 14 °C while
heating its bottom to 60 °C [Fig. 2(d)]. The temperature
difference drops across the glass-water-glass chamber
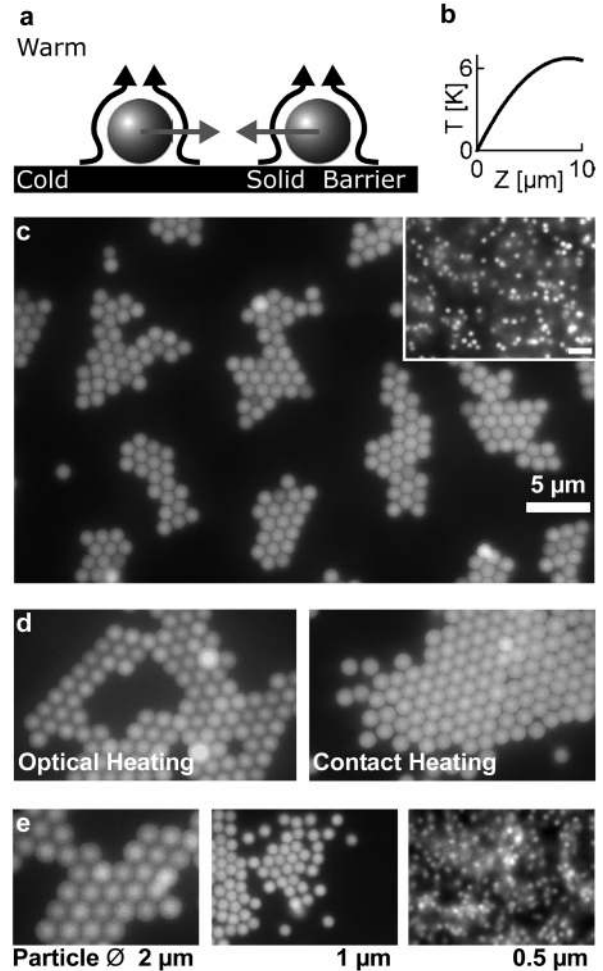sandwich according to their respective thickness and heat

FIG. 2.   *Thermophoretic crystallization.* (a) In a strong tem-
perature gradient, particles move ballistically to the cold surface
(side view). The persisting slip flow is deflected by the surface
and leads to mutual hydrodynamic attraction. (b) Temperature
profile. (c) Colloidal crystals of 1 μm polystyrene particles on a
cold surface for positive Soret coefficients (view from the top
after 20 s of heating). Inset: Before temperature application.
(d) Crystals form equally well for a contact heated chamber
without laser irradiation (2 μm particles). (e) At a fixed tem-
perature gradient of 0.28 K/μm, crystallization strongly de-
pends on the Soret coefficient, following the threshold
condition of Eq. (1). See supplemental material [34].

conductivities and subsequently lifts the particles against
sedimentation. We calculated a temperature gradient of
0.05 K/μm, slightly smaller than the optically applied
gradient of 0.28 K/μm but still within the criterion (1).
We find less densely packed crystals for 2 μm polystyrene
particles under contact heating as expected from the
weaker temperature gradient.

Size dependence.—As seen in Fig. 2(e), a thermal gra-
dient of $\nabla T = 0.28$ K/μm applied to particles of different
sizes caused strong varying degrees of attraction. Particles
with 2 μm diameter ($S_T = 43$ K^{-1}) experienced high at-
traction to one another; moderate attraction was observed
for 1 μm particles ($S_T = 20$ K^{-1}); no attraction was seen

for 0.5 μm particles ($S_T = 4$ K^{-1}). We found crystalliza-
tion only when the criterion of Eq. (1) was fulfilled, where
the values $\nabla T a S_T$ for the respective particle size were 12,
2.8, and 0.28.

Quantification of the attraction.—In a thermal gradient
of 0.28 K/μm, we determined the attractive pseudo-
potential of a particle pair by tracking the interparticle
distance distribution parallel to the surface. The usage of
"pseudo" should imply that the forces are not conservative
[23]. Figure 3(a) shows an image of the isolated 2 μm
polystyrene particles, which were tracked ($S_T = 43$/K, F-
8827, Molecular Probes) and found to fluctuate in close
proximity. We obtained the pseudopotential difference ΔV
of the attraction from the Boltzmann distribution. The
number of particles ΔN found within the distance interval
$[d, d + \Delta d]$ is given by

$$\Delta N(d) = 2\pi d \bar{N} e^{-\Delta V(d)/kT} \Delta d, \qquad (2)$$

with average particle density $\bar{N}$ [24]. Particle distances
were recorded over 1300 s and included stochastic binding
and unbinding processes of the particle pair. The resulting
pseudopotential $\Delta V(d)$ from $N = 8300$ pair distance val-
ues is plotted in Fig. 3(b). The pseudopotential is shifted to
zero potential at a distance of 8 μm. Beyond this distance,
we did not obtain enough data to statistically evaluate the

a

b

c

0.4   0.6   0.8   1.0   1.2
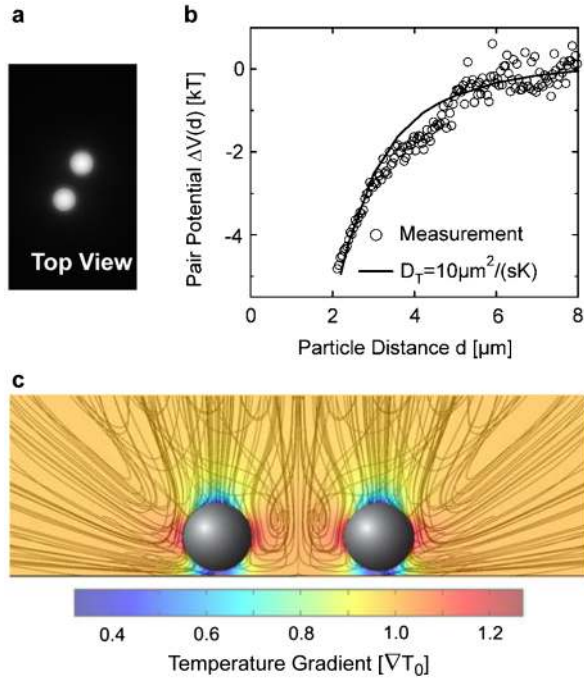Temperature Gradient [∇T_0]

FIG. 3 (color online). *Particle attraction from thermophoretic
slip flow.* (a),(b) The distance distribution of a single particle pair
is measured by particle tracking. The effective pseudo pair
potential $\Delta V(d)$ was determined using Boltzmann statistics
(open circles). (c) The three-dimensional flow around the parti-
cles was calculated using finite elements. A projection of the
flow lines is shown in gray; the thermal gradient is color coded
and given in units of the free solution temperature gradient ∇T_0.
The calculated pair potential is plotted as a solid line in (b).

shape of the curve. The attraction well reaches a depth of
5 kT.

Slip-flow boundary condition.—Slip-flow conditions in
the Debye layer close to the surface of the particles have
been proposed by Ruckenstein [11] and discussed by sev-
eral authors, including Keyes [12], Anderson [13],
Morozov [14], Semenov [15], Piazza [16], and Würger
[17]. The details of the provided flow fields vary. We will
compare our experiments with the flow fields of Piazza and
Würger. The authors differ in their treatment of flow at the
nanoscale and assume either nonslip flow (Piazza) or qua-
sislip flow (Würger) at the particle-water interface inside
the Debye layer. Both solutions are identical for distances r
larger than the Debye length λ and for particles with radius
$a \gg \lambda$, which is in the regime probed by our experiments.

The Marangoni force tangential to the surface counter-
balances the off-diagonal components of the hydrody-
namic surface stress [17]. In Cartesian coordinates
(x, y, z), the tangential direction at the surface of the sphere
is $\mathbf{t} = (-xz, -yz, x^2 + y^2)/(r\sqrt{x^2 + y^2})$ and the normal di-
rection $\mathbf{n} = (x, y, z)/r$. With $r = \sqrt{x^2 + y^2 + z^2}$ and the fluid
velocity $\mathbf{v}$, the surface boundary condition reads explicitly

$$\eta[r\mathbf{n} \cdot \nabla(\mathbf{t} \cdot \mathbf{v}/r) + \mathbf{t} \cdot \nabla(\mathbf{n} \cdot \mathbf{v})] = \gamma_T \mathbf{t} \cdot \nabla T. \qquad (3)$$

The temperature dependence of the surface energy given
by $\gamma_T = 3\eta D_T/a\kappa$ is set to match the thermophoretic
mobility D_T in free solution within the pseudoslip condi-
tion framework. The factor $\kappa = (3\kappa_S)/(2\kappa_S + \kappa_P)$ is given
by the thermal conductivities of water $\kappa_S = 0.54$ W/(m ·
K), polystyrene $\kappa_P = 0.13$ W/(m · K), and fused silica
$\kappa_P = 1.3$ W/(m · K). The thermophoresis of particles
was measured by single particle tracking [8] at similar
thermal gradients. The treatment with nonslip in the
Debye layer [16] gives the same simulation result.
However, it requires a different microscopic parametriza-
tion for γ_T to match the measured values of D_T.

Finite element calculation.—We carried out the simula-
tion using an industrial finite element solver in 3D
(FemLab 3.1, Comsol). Nonslip boundary conditions were
used at the bottom sapphire surface. The surrounding box
was treated with symmetric boundaries at the symmetry
plane between the spheres and neutral flow boundary con-
ditions otherwise. The temperature gradient was calculated
using bulk thermal conductivities of the materials. The
particle was located above the bottom sapphire at the sedi-
mentation length kT/F with a downward force F from
thermophoresis and gravitation. We iteratively adapted the
surface slip-flow condition to meet Eq. (3) within a relative
error of 10%. The flow lines and the thermal gradient for a
solution with a particle distance of 4.6 μm are depicted in
Fig. 3(c). A simulation of a single particle without nearby
surfaces reproduced the analytical drift solution of
Ref. [17].

We calculated the total hydrodynamic forces on the
surfaces $d\Omega$ of one particle, which is subjected to the fluid
flow, induced by a second particle. The x component of the

total hydrodynamic force F_x is given by

$$F_x = \int \left[\eta \mathbf{n}\left(\nabla v_x + \frac{\partial}{\partial x}\mathbf{v}\right) - n_x p \right] d\Omega, \qquad (4)$$

with the pressure p, viscosity η, velocity field $\mathbf{v}$, and normal vector $\mathbf{n}$ [25]. By integrating $F_x(d)$ for a set of particle distances d, we obtained the pseudopotential of the particle attraction $V(d)$. Both the experimentally and theoretically obtained pseudopotentials flatten out into noise levels for distances beyond 8 μm. As shown in Fig. 3(b), the calculated pseudopotential fits the experimentally determined potential in ample detail without fitting parameters. Thus the particle attraction can be quantitatively understood based on the hydrodynamic interaction induced by thermophoretic slip flows.

Discussion.—Particle attraction is not expected from a thermodynamic viewpoint of thermophoresis. As the thermally insulating particles are not heated by laser absorption, we find 100-fold smaller thermal gradients parallel to the surface compared to the perpendicular gradient, as calculated from heat conduction [Fig. 3(c)]. These residual parallel gradients would lead to a minor thermophoretic repulsion for $S_T > 0$ in contradiction with the attractive forces found experimentally.

The reported hydrodynamic attraction differs fundamentally from previously reported experiments [26]. There, thermal convection was externally triggered and particle crowding lead to crystallization. Comparable colloidal crystals from large scale fluid flow were also found at the chamber surface after experiments on thermodiffusion-assisted convection [27]. In contrast, we report particle attraction solely driven by a highly localized flow from the particles under convection-free conditions. The driving mechanism also differs from hydrodynamic attraction in sedimentation [28,29] or during electrophoretic deposition [30–32], where the mutual attraction is predominantly driven by an electro-osmotic fluid flow at the barrier surface [32] rather than on the particle surface. The reported particle attraction in a thermal gradient is likely to disturb thermal field flow fractionation for large particles [18]. Temperature gradients on a surface can be structured by patterning the thermal conductivity of the substrate, allowing for considerable technical applications such as the formation of photonic crystals [33] or biomolecule detection.

Conclusions.—At sufficiently large temperature gradients, we found direct evidence for slip-flow models of thermophoresis. Ballistic thermophoretic drift frustrated by a solid wall leads to interparticle attraction in contrast to thermodynamic expectations. As a result, we were able to create two-dimensional crystals thermally. Marangoni-like slip flow at the particle surface describes the attraction force quantitatively. Our finding argues towards two regimes in thermophoresis depending on the applied temperature gradient.

*dieter.braun@physik.lmu.de

[1] C. Ludwig, Sitz.ber. Akad. Wiss. Wien, Math.-Nat.wiss. Kl. **20**, 539 (1856).
[2] C. Soret, Arch. Sci. **3**, 48 (1879).
[3] S. R. de Groot and P. Mazur, *Non-Equilibrium Thermodynamics* (North-Holland, Amsterdam, 1969).
[4] J. K. G. Dhont, J. Chem. Phys. **120**, 1632 (2004).
[5] J. K. G. Dhont, J. Chem. Phys. **120**, 1642 (2004).
[6] S. Fayolle *et al.*, Phys. Rev. Lett. **95**, 208301 (2005).
[7] S. Duhr and D. Braun, Phys. Rev. Lett. **96**, 168301 (2006).
[8] S. Duhr and D. Braun, Proc. Natl. Acad. Sci. U.S.A. **103**, 19 678 (2006).
[9] R. D. Astumian, Proc. Natl. Acad. Sci. U.S.A. **104**, 3 (2007).
[10] J. K. G. Dhont *et al.*, Langmuir **23**, 1674 (2007).
[11] E. Ruckenstein, J. Colloid Interface Sci. **83**, 77 (1981).
[12] T. Keyes, J. Stat. Phys. **33**, 287 (1983).
[13] J. L. Anderson, Annu. Rev. Fluid Mech. **21**, 61 (1989).
[14] K. I. Morozov, J. Exp. Theor. Phys. **88**, 944 (1999).
[15] M. E. Schimpf and S. N. Semenov, J. Phys. Chem. B **105**, 2285 (2001).
[16] A. Parola and R. Piazza, Eur. Phys. J. E **15**, 255 (2004).
[17] A. Würger, Phys. Rev. Lett. **98**, 138301 (2007).
[18] P. M. Shiundu, G. Liu and J. C. Giddings, Anal. Chem. **67**, 2705 (1995).
[19] J. Rauch and W. Köhler, Phys. Rev. Lett. **88**, 185901 (2002).
[20] D. Braun and A. Libchaber, Phys. Rev. Lett. **89**, 188103 (2002).
[21] M. Braibanti, D. Vigolo, and R. Piazza, Phys. Rev. Lett. **100**, 108303 (2008).
[22] F. M. Weinert *et al.*, Phys. Rev. Lett. **100**, 164501 (2008).
[23] T. M Squires, J. Fluid Mech. **443**, 403 (2001).
[24] D. Rudhardt, C. Bechinger, and P. Leiderer, Phys. Rev. Lett. **81**, 1330 (1998).
[25] L. D. Landau and E. M. Lifshitz, *Fluid Dynamics* (Elsevier Butterworth-Heinemann, Oxford, 2004).
[26] S. Duhr and D. Braun, Appl. Phys. Lett. **86**, 131921 (2005).
[27] R. Cerbino, A. Vailati, and M. Giglio, Phys. Rev. E **66**, 055301 (2002).
[28] T. M. Squires and M. P. Brenner, Phys. Rev. Lett. **85**, 4976 (2000).
[29] J. Bafaluy *et al.*, Phys. Rev. Lett. **70**, 623 (1993).
[30] M. Giersig and P. Mulvaney, Langmuir **9**, 3408 (1993).
[31] M. Trau, D. A. Saville, and I. A. Aksay, Science **272**, 706 (1996).
[32] W. D. Ristenpart, I. A. Aksay, and D. A. Saville, Phys. Rev. E **69**, 021405 (2004).
[33] Y. A. Vlasov *et al.*, Nature (London) **414**, 289 (2001).
[34] See EPAPS Document No. E-PRLTAO-101-036841 for a movie related to Fig. 2. For more information on EPAPS, see http://www.aip.org/pubservs/epaps.html.